Particle Accelerators, 1972, Vol. 4, pp. 111–126

ACCELERATING TESTS ON THE FIRST SECTION OF THE KARLSRUHE SUPERCONDUCTING PROTON ACCELERATOR

A. BRANDELIK, A. CITRON, P. FLÉCHER, J. L. FRICKE, R. HIETSCHOLD, G. HOCHSCHILD, G. HORNUNG, H. KLEIN,† G. KRAFFT, W. KÜHN, M. KUNTZE, B. PIOSCZYK, E. SAUTER, A. SCHEMPP,† D. SCHULZE, L. SZECSI, J. E. VETTER AND K. W. ZIEHER

Institut für Experimentelle Kernphysik, Kernforschungszentrum und Universität Karlsruhe, Germany

This report is a summary of recent tests made on the first section of the Karlsruhe superconducting linear accelerator. The following elements were assembled: Cockcroft–Walton injector, chopper-buncher system, and first cryostat. The cryostat contained the first accelerating section and a superconducting quadrupole doublet while dummy sections were placed in the position of the second and third tanks and the second quadrupole doublet, allowing the beam to traverse the entire length of the cryostat. These tests were carried out in March and June 1972. The design field of $E_{axis}^{TW} = 1.155$ MV/m was obtained in stable operation. At an injection energy of 750 keV and the design field on the axis a maximum energy gain of 380 keV was measured with a continuous proton beam.

1. INTRODUCTION

A superconducting linear accelerator is not only of interest for basic nuclear research, but also for biological and radiotherapy applications. This is based on the possibility to generate high currents of secondary particles with superior beam quality compared to conventional linacs. This is due to the fact that in a superconducting linac, continuous operation becomes possible at relatively high energy gradients per unit length, avoiding space charge and transient effects.

More and more laboratories concentrate their effort on the field of rf superconductivity. A superconducting electron accelerator is under construction at Stanford (USA).[1] A superconducting microtron is performing at Urbana (USA).[2] Moreover the aspects of a superconducting heavy ion machine are investigated at Cal Tech,[3] at Argonne,[4] and at Oak Ridge[5] most recently. There are also ideas in Germany to use rf superconductivity for the acceleration of heavy ions. Basic development work on superconducting rf cavities has been done at Stanford (HEPL),[6] at SLAC,[7] at Paris,[8] at Brookhaven[9] and at Karlsruhe[10] in the past five years.

The objectives of the accelerator program at Karlsruhe are to demonstrate the feasibility of a superconducting π-meson factory. The possibilities of such a superconducting linear accelerator in the energy region of 500 MeV must be compared to the latest conventional 'π-meson factories'. A conventional π-meson factory is operational at Los Alamos (USA),[11] one is under construction at Villigen (Switzerland) and Vancouver, BC. The possibilities of a 'superconducting π-meson factory' are expected to be superior to both of them, although a quantitative prediction is not possible at the moment. The pilot linac under construction will give the opportunity to solve all the technical problems and to make reliable cost estimates possible.

The principal feature which distinguishes linear ion and proton accelerators from electron accelerators is the difference in particle speed. As a consequence, the accelerating structure is substantially more complicated for a proton accelerator. For all ion accelerators an optimum frequency much lower than for electrons is used. Also the radial defocusing effects require auxiliary focusing elements. Low frequency and more quadrupole focusing elements aggravate the application of rf superconductivity appreciably. We decided to start at an injection energy of 750 keV, where a normal Cockcroft-Walton cascade is conveniently used. We chose a superconducting helically-loaded structure, for which the difficulties mentioned are less severe.

† Institut für Angewandte Physik der Universität Frankfurt, Germany.

FIG. 1. View at the proton injector (Cockcroft–Walton) for 750 keV and a continuous proton current of 2 mA.

The radial dimensions (90 MHz) are small (helix radius 4 cm) in spite of a low frequency and a large acceptance.[12] The basic plan of the Karlsruhe accelerator was given in a status report by Citron.[13] The work on the helix accelerator is a collaborative effort of the Karlsruhe accelerator group and a group at the University of Frankfurt under Klein.[14] Later on the helix accelerator will be followed by another type of accelerating structure which should be operated at a higher frequency. Thereby, we can study the problems of the frequency jump and beam matching. In this way all problems occurring in a larger accelerator will be faced.

2. EXPERIMENTAL ARRANGEMENT

2.1. *Injector*

The injector was delivered by Tunzini–Sames (Grenoble). It is an open air cascade (800 keV) with electrostatic screening at a distance of 2.5 m from the high voltage electrodes. The total volume occupied is 15 m × 8 m × 8 m. The cascade consists of 3 parts: the cascade generator, a filter column, and the accelerating column. The latter contains 20 stages of a vertically mounted beam tube (Fig. 1).

To suppress secondaries, which yielded a large amount of X-rays, a deflecting system consisting of permanent magnets in each stage has been included. Without beam a gas pressure of about 2×10^{-6} Torr is obtained in the whole tube, but during operation of the ion source, the pressure increases up to 5×10^{-5} Torr at the upper end.

The injector was installed at Karlsruhe in the summer of 1971. A comprehensive program of performance tests were made until the end of 1971. Up to now, no external high voltage breakdowns along the accelerator tube and along the supporting columns or from any high voltage point to ground potential have been observed. But internal breakdowns occurred, depending upon gas pressure.

At present, the proton current is limited by internal breakdowns which occur in the range between 1.5 and 2 mA. The performance tests were carried out mainly at 1 mA, though temporary currents up to 2 mA have been obtained.

At a current of 1 mA and 850 keV, the emittance of the proton beam was measured. The normalized emittance was 0.072 cm × mrad for 80 per cent of the beam. Extrapolation from 1 to 2 mA with the measured current dependence leads to an emittance of 0.12 cm × mrad close to the design value of 0.10 cm mrad.

2.2 *Chopper-buncher System*

A chopped and tightly bunched beam with clean interspaces is necessary for the transition to another structure at the end of the helix. A chopper-buncher system for 750 keV and 90 MHz has been developed. The energy is modulated twice by two gaps of the same normal conducting rf resonator at the helix frequency. Between two transitions the beam passes through a 270° deflecting magnet for chopping. The scheme is described in more detail elsewhere.[13,15] The design energy modulation of 2.3 per cent was obtained at an rf input power of 4 kW. The operation was stable without uncontrolled temperature rise at the rf coupling probes. But the system failed during the tests described here due to trivial reasons. Therefore, in the accelerator experiments only a dc beam was obtained and injected into the first helix section.

2.3. *Focusing*

The first few focusing lengths at low energy are rather short (~50 cm). In order to minimize the technical accelerator length, we chose superconducting quadrupole lenses. Magnetic fields are shielded from the cavities by superconducting Pb screening. Moreover, the quadrupoles will be energized after the accelerating cavities have become superconducting. A first quadrupole doublet has been built by Siemens (Erlangen) and is included in the cryostat. The design values are: gradient 30 T/m, length 30 cm, aperture 6 cm. A superconducting switch permits disconnection of the quadrupoles from the power supply after energizing.

2.4. *Accelerating Structure*

The helix section is similar in concept to that described by Citron.[13] Different independent subsections are aligned with quadrupole lenses in between, inserted into the cryostat as a whole.

Each helix subsection is built of $\lambda/2$ niobium helices. The geometry parameters for the first section were established by Klein and his group.[16] For the first three accelerator cavities, the outer tank is fabricated of electroformed copper with

integrated cooling channels and then plated with lead. The helices, their support and cooling and the coupling devices form a rather complicated structure which was electron-beam-welded into a single niobium part named 'Deckel'. This is then bolted to the copper tank. Details of construction and preparation fo the first section are given in Sec. 3.

2.5. *Rf System*

The design of the rf system has to take into account two facts especially valid for the helix. First, mechanical oscillations induced by external forces modulate the electrical resonant frequency.[17] From laboratory experiments, modulation frequencies between 20 Hz and 50 Hz with a frequency stroke in the range of a few kHz were expected. Secondly, the rf itself can induce oscillations due to ponderomotive forces (radiation pressure).[18] Different precautions in different orders of complexity are possible: First a mechanical isolation of the cryostat from floor level and helium transfer lines has to be included and should give a screening factor up to 10 for external perturbations. Secondly, the remaining frequency modulation has to be reduced by a fast tuning device which is designed to handle reactive powers up to 10 kVA. Such a tuning device using pin diodes has been developed at Karlsruhe, but has not been tested so far.[19] Less economical but also less complicated would be an external load to broaden the bandwidth of the superconducting cavity. Finally, an amplitude and phase control system similar to that of a conventional linac has to be provided.

No attempt was made in the first accelerator tests to demonstrate the capability of operation at a fixed frequency. For this reason, the first cavity was not equipped with either slow or dynamic frequency tuners. The rf generator frequency was tuned to the frequency of the helix subsection by a phase sensitive frequency lock-in. It was shown in preceding experiments with a single helix that the parameters of the frequency loop can be chosen so as to guarantee stability against ponderomotive effects.[20,21] The electromechanical forces cause an appreciable static frequency shift of the helix resonator which is proportional to the square of the electrical field strength. Therefore, the capture range of the frequency loop should be broadened sufficiently, and the rf amplifiers used should be broad enough to avoid phase lag. Amplitude and phase stability can be obtained by using only the frequency control circuit with high loop gain but an auxiliary amplitude loop is advantageously used.

The rf circuit used in these first accelerator tests is given in Fig. 2.

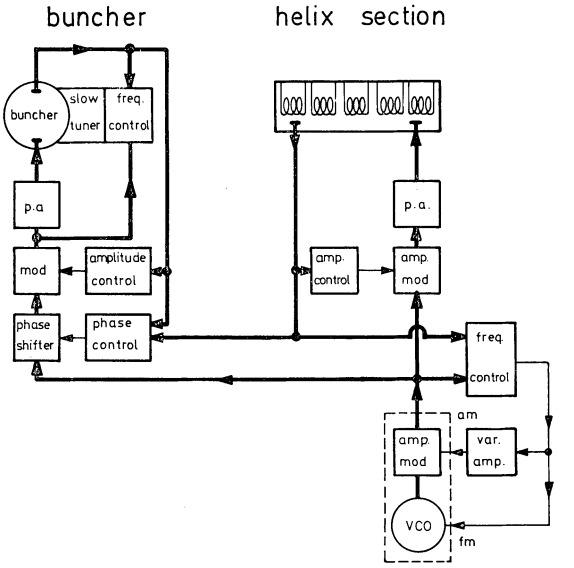

FIG. 2. Circuit diagram of the frequency control system for buncher and first helix section.

2.6. *Cryogenic System*

The cryogenic system of the accelerator consists so far of the helium refrigerator, helium pipelines, and one cryostat. The refrigerator was delivered by Linde[22] (München) and can remove nearly 380 W at 1.8 K. It was successfully tested and used in other experiments before. The helium transport lines are vacuum isolated and are about 15 m long. The total thermal loss is almost 20 W.

The basic idea of the cryostat design was to use a double vacuum system, avoiding leaks between the ultra-high vacuum in the accelerating system and the helium bath.[23,24] Liquid helium is guided in cooling channels only, which are connected to a pair of helium storage pipes (twin pipes) inside the cryostat (Fig. 3). Cooling is achieved by heat transfer in helium II without mass transport, i.e. only by the 'internal convection' mechanism of superfluid helium.[25]

Cold flanges have to be leaktight only between the beam vacuum of $<10^{-8}$ Torr and isolation

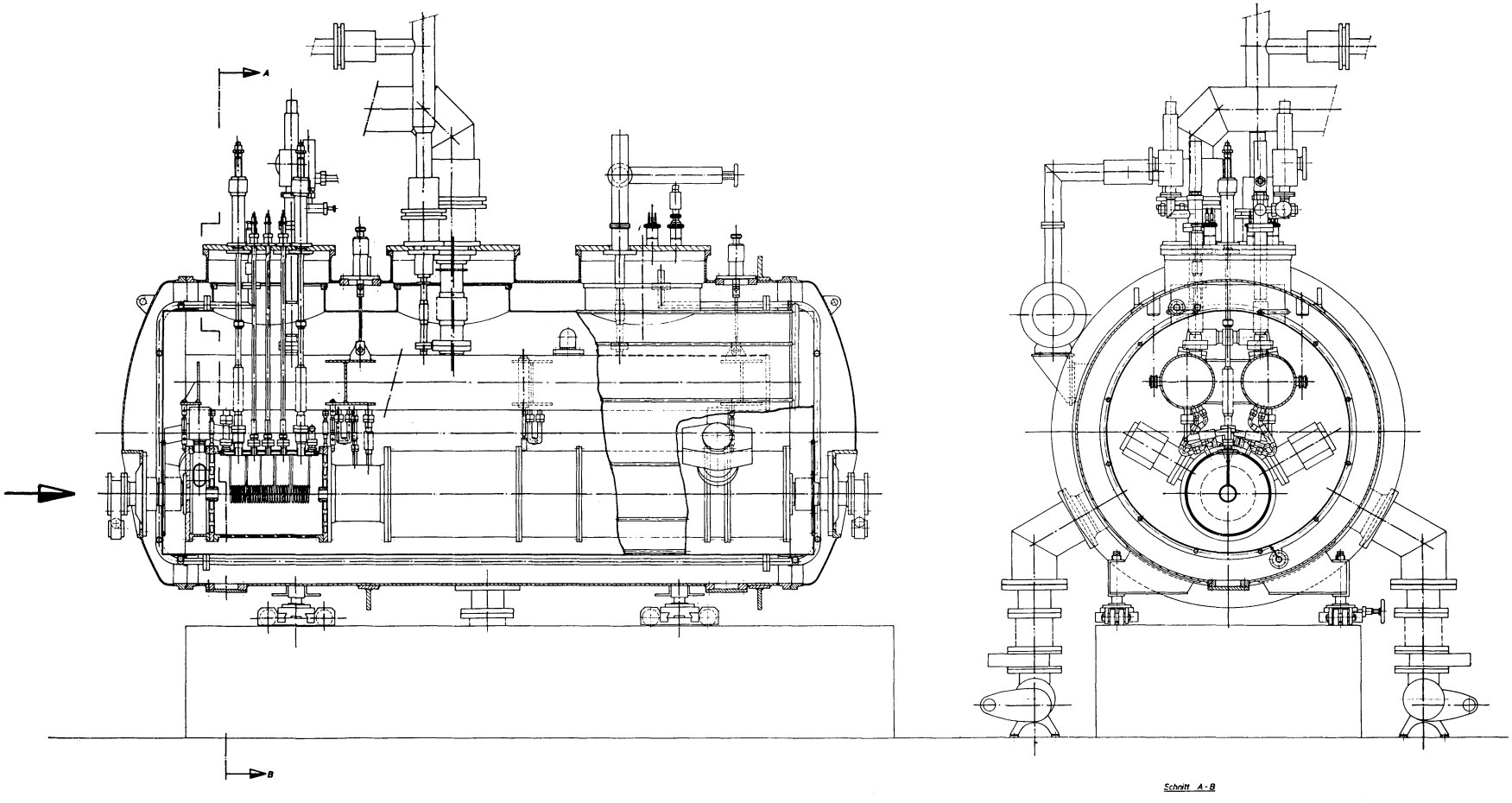

FIG. 3. Drawing of the experimental arrangement. The proton beam enters at the valve from the left, traverses a pumping section, the superconducting helix section, the quadrupole doublet and some dummy sections, and is analyzed after exit of the cryostat at the right side.

vacuum of 10^{-6} Torr, whereby the requirements and the chances of failure are strongly reduced. Turbomolecular pumps are used for isolation vacuum; the gas pressure is designed to be less than 10^{-6} Torr. It is important to obtain good beam vacuum conditions before cooldown. Ion getter pumps (Ultek) are used to obtain the beam vacuum. The ion pumps can still be operated at liquid nitrogen temperature after cooldown (first experimental run). This was demonstrated in test experiments.[26] A liquid nitrogen shield is inserted in the cryostat to reduce heat radiation from room temperature parts. Electrical and rf feedthroughs from room temperature to the accelerating system are thermally tied to the liquid nitrogen shield to reduce thermal losses. For the same reason superinsulation (12 layers) on the twin pipes and on the structure part are used. The complete accelerating system is suspended from the twin pipes which are directly connected to the refrigerator by the external helium transport lines.

The first cryostat is a 3 m module fabricated of stainless steel and aluminum (Fig. 4). It is designed to contain 3 helix subsections and 2 quadrupole lenses. In this experiment, dummy sections replaced the second and third helix subsections and the second quadrupole lens. The over-all thermal losses of the loaded cryostat were determined by helium boil-off measurements. The total evaporation losses were about 15 W. The rf losses of the superconducting helix subsection are of the order of several watts.

2.7. *Energy Analysis*

After acceleration, beam analysis was done with a magnet at the exit of the cryostat. In a first setup the magnetic deflection of the beam was observed on a fluorescent screen as the field was changed and

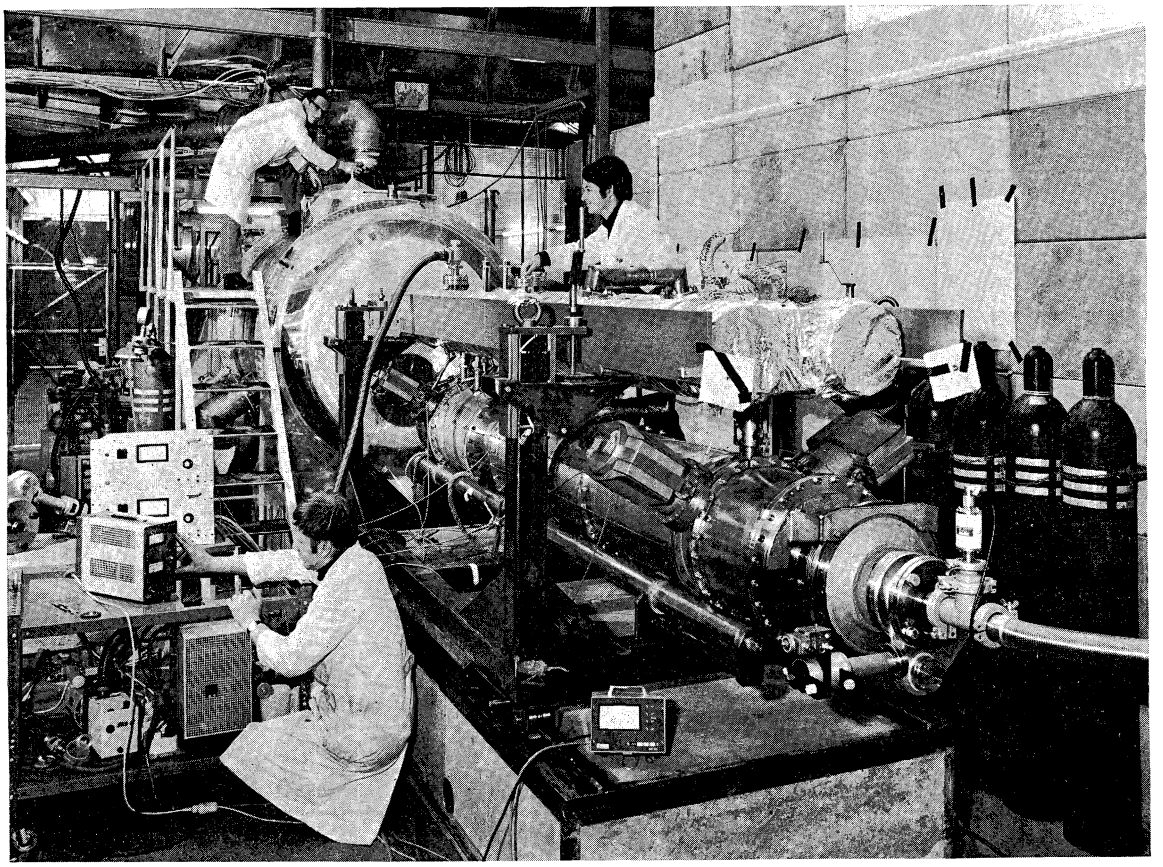

FIG. 4. Photograph of the inner part of the cryostat (see Fig. 3) looking from the downstream end, taken during final assembly in March 1972.

reversed. The energy distribution was determined by replacing the fluorescent screen by a wire positioned at a fixed angle of deflection and measuring the collected current while varying the magnetic field.

3. CONSTRUCTION AND PREPARATION OF THE FIRST RESONANT CAVITY

Earlier experiments in the laboratory with a a single niobium helix in a lead-plated outer conductor have shown that fields $\geqq 500$ G and Q's of about 10^8 could be obtained reproducibly.[27] In the meantime, improved maximum field strengths $\geqq 1000$ G have been obtained in a full niobium helically-loaded cavity of smaller size.[28] But for the design of the first coupled array of 5 helices, the combined lead/niobium technique has still been used, because the concept of integrated cooling channels can easily be realized for electroformed copper cylinders. To decrease the fields at the lead surfaces, a ratio of resonator to helix radius of $b/a = 5$ was chosen. The helices were designed for an axial field strength of $E_0 = 1.155$ MV/m, giving maximum surface fields of $E_z = 15$ MV/m and $H = 437$ G. The parameters of the five $\lambda/2$ helices were found balancing the arguments of radial acceptance, phase acceptance, shunt impedance and cooling possibility, and keeping peak electric fields at a value where field emission loading is still tolerable. Available niobium tube size, minimum bending radius and tolerances of the pitch further restricted the choice of parameters. The final parameters of the coupled array of helices are given in Table I. To determine maximum field strengths, the ring model calculations of Siart[29] have been used. To correct for end field effects, a method according to Schempp[30] has been taken. Flatness and resonant frequency were checked and adjusted in a room-temperature model tank.

The construction of the first section of the helix accelerator is shown schematically in Fig. 5. All niobium parts are electron-beam-welded into a single niobium piece ('Deckel'). The electron-beam-welding was done by Siemens (Erlangen). In the middle of each helix, a coupling tube penetrates through the 'Deckel', giving two movable and three fixed probes access to the E_r fields. The 'Deckel' with the suspended helices is flanged into the lead-plated copper tank. Rf contact is made by a knife edge, whereas vacuum sealing at room temperature is achieved by a perbunan ring. The same kind of sealing is used to attach the end plates to the cylindrical part. The 'Deckel'—filled with liquid helium and forming a helium bath for the suspended helices—is connected with the main helium reservoir within the twin pipes by two tubes with an inner diameter of 3 cm.

TABLE I

Parameters of the first helix section

Frequency at room temperature	at low power	90.77 MHz
Frequency at 1.8	at low power	90.92 MHz
Injection energy		0.75 MeV
Design field on the axis E_{axis}^{TW}		1.155 MV/m
Static frequency shift at design field		690 kHz
Peak electric field E_z^p		15 MV/m
Peak magnetic field H_r^p		437 G
Number of helices		5
Length of a $\lambda/2$ helix		7–9 cm
Pitch of helices	about	1 cm
Radius of helices		3.7–4.2 cm
Radius of outer cylinder		20 cm
Electrical length of coupled array		36.8 cm
Length of outer cylinder		58.5 cm
Energy gain at design field for continuous beam		424 keV

Preparation of the 'Deckel' was done in several steps. The bottom plate of it was premachined, stress relieved at 1000 °C, and machined to the final tolerances. Coupling tubes and helium supply were machined separately. The helices were wound on mandrils with different diameter, using 3 m long tubes of 6.3 mm diameter and 0.75 mm thickness. The material (from Kawecki and Fansteel) was first mechanically polished. Then, the helices were annealed at 1200 °C and subsequently electropolished in a solution of H_2SO_4 (97 per cent) and HF (40 per cent) with a volume ratio of 85 : 10, removing 30 μm of niobium. The coils were then cut to the right dimensions and the ends, which serve as suspension tubes, were straightened. After a stress relieving process, the pitch of the helices was corrected. They were then anodized in 12.5 per cent NH_3 to protect the surface during the following manipulations. To prepare superconducting Nb surfaces by electropolishing and subsequently anodizing is a relatively new method, which has been developed in the research work on superconducting cavities at Erlangen[31] and at Karlsruhe.[10,32]

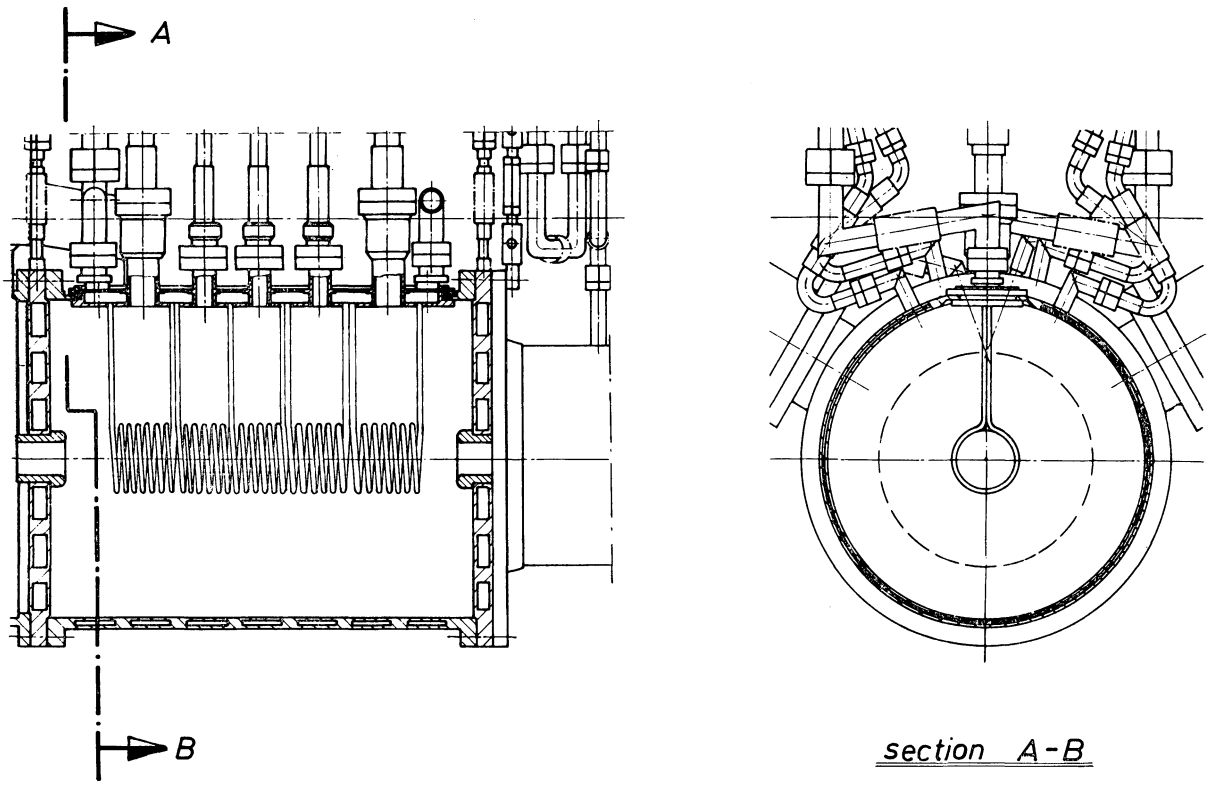

FIG. 5. Drawing of the first helix section with Nb 'Deckel' and rf coupling probes.

In the model tank, the positions of the helices with respect to one another could be varied. In this way the final positions of the helix suspensions were found and the corresponding bore holes could be machined into the 'Deckel'.

Electron-beam-welding of the different niobium parts was then carried out in the following steps:

—the helium tubes were welded to the cover plate, and the rf coupling tubes to the bottom plate of the 'Deckel'.
—the helices were welded into the bottom part.
—the cover plate and bottom part were welded together, including the welds around the coupling tubes on top of the 'Deckel'.

Before the second step the bottom part was electropolished (about 20 μm) and the oxide film used for protection was removed from the helices for welding.

The finished 'Deckel' was flanged into the copper tank and flatness, as well as resonance frequency, was checked. Minor displacements gave a final resonance frequency of 90.46 MHz at room temperature. Figure 6 gives a photograph of the finished helix section.

Immediately before the final assembly, the whole 'Deckel' was electropolished again (about 20 μm), and anodized (250 Å). At the same time, the copper tank was freshly lead-plated. Mounting the section and the rf coupling took about one hour. The section was then evacuated through the beam tubes and was kept under a vacuum of 10^{-5} Torr during the assembly of the cryostat, except that it was necessary to interrupt the vacuum preceding period A1 (see Sec. 4.3.).

Preceding period B1 similar treatments were performed: the oxide layer was removed in HF and the helices were electropolished about 20 μm. Finally, the helices were anodized in 0.1 NH_5SO_4 (400 Å).

4. RESULTS OF THE ACCELERATING TESTS

4.1. *Experimental Procedure*

The results summarized in the following have

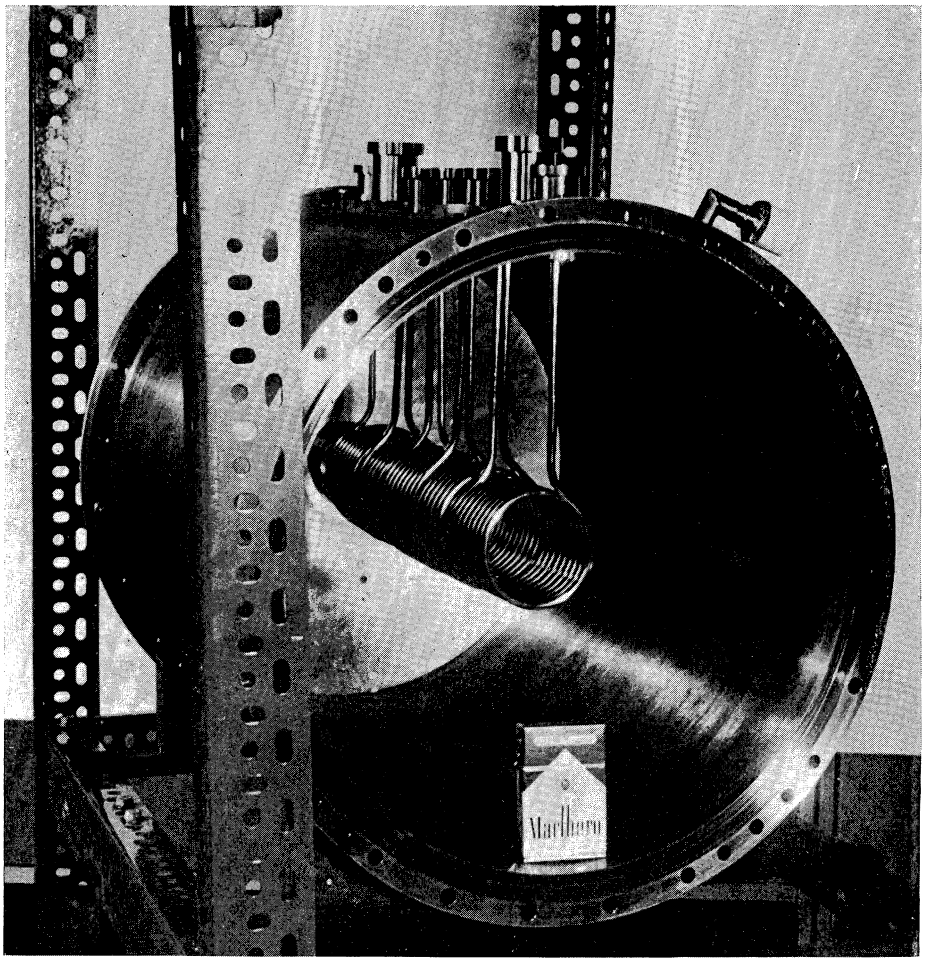

FIG. 6. Photograph of the finished helix section briefly before final surface preparation.

been obtained during different experimental periods:

A1	March	6–March	17
A2	March	20–March	24
B1	June	12–June	17
B2	June	20–June	28
B3	June	30–July	7

The first experimental period A1 was interrupted after two weeks of operation (day and night) for additional tests on the cooling system. It was continued during period A2 after warming up the cryostat to room temperature and subsequently cooled down again without any changes. The second experimental run started with the period B1, where a freshly prepared superconducting cavity, an improved rf system and a slightly changed cooling system were used. This period was interrupted after 10 days of operation due to a failure of the refrigerator. The cryostat warmed up to LN_2-temperature, this time, and the experiment could be continued with the period B2 after 3 days. Due to an accidental vacuum breakdown of the cold cryostat it was interrupted once more, because the Q-value was deteriorated. The cryostat was consequently warmed up to room temperature and cooled down again after 24 hours of pumping. The experimental run was continued with the period B3.

The experimental results can be divided rather conveniently into several subdivisions. These are rf properties of the cavity, feed-back and control system, operation of the cryogenic system, and experiments with the proton beam.

4.2. *Rf Properties of the Cavity*

Rf measurements were done using the experience gained in laboratory experiments. The Q-values at low fields were determined from decay time of stored energy. In the range of high power levels Q-values were obtained from power loss in the

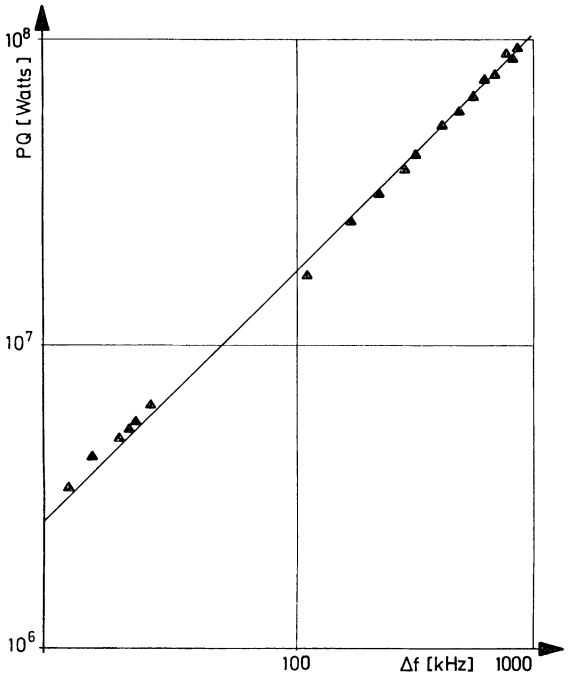

FIG. 7. Results of calibration measurements: stored reactive power $P_c \times Q_0'$ in the first helix section as function of static frequency shift Δf.

cavity P_c and corresponding static frequency shift Δf (see Sec. 2.5): Δf is proportional to $P_c \times Q_0'$, where Q_0' includes coupling losses. Calibration measurements give (Fig. 7)

$$\Delta f/\mathrm{kHz} = 5.7 \times 10^{-6} \times P_c Q_0'/\mathrm{W} \qquad (1)$$

with an experimental error <5 per cent.

Stored energy and all fields in the cavity are uniquely related to the easily accessible quantity Δf, as in the case of a single helix.[28]

Perturbation measurements on this helix section at room temperature result in

$$E_{\mathrm{axis}}^{\mathrm{TW}}/\mathrm{MV/m} = 1.05 \times 10^{-4} \sqrt{P_c Q_0'}/(\mathrm{W})^{1/2} \qquad (2)$$

where the estimated error in E is 5 per cent. Combining Eqs. (1) and (2) gives

$$E_{\mathrm{axis}}^{\mathrm{TW}}/\mathrm{MV/m} = 4.38 \times 10^{-2} \sqrt{\Delta f}/(\mathrm{kHz})^{1/2} \qquad (3)$$

Peak fields were calculated according to the ring model for long helices. The result is, that E_z and H_r of the second helix determine the peak fields of this coupled array of helices. The relations between peak fields and accelerating field on the axis are

$$E_z^{\mathrm{P}} = 12.85 \times E_{\mathrm{axis}}^{\mathrm{TW}} \qquad (4)$$

$$H_r^{\mathrm{P}}/\mathrm{G} = 378\, E_{\mathrm{axis}}^{\mathrm{TW}}/\mathrm{MV/m} \qquad (5)$$

The existing multipactoring barriers could be overcome by 'processing'. A broad barrier extending from $\Delta f = 25$ kHz to $\Delta f = 105$ kHz took approximately 15 hours' processing time. The measured r-factor[33] was about 100, indicating one point multipactoring. Multipactoring barriers reoccurred after warming up to room temperature in periods A2 and B3.

Q-values as function of field strength are summarized in Fig. 8. The principal characteristic is known from preceding single helix experiments.[28] Starting with a Q-value 10 times lower than in single helix experiments at low power levels, the high field Q-value saturates at 3.3×10^7 in period A1 and period B3. This value is about a factor of 4 lower than in single helix experiments. The reasons for this Q-behaviour are not known. The obtained high field Q corresponds to an improvement factor of about 2×10^4, compared to room-temperature copper.

Between periods A1 and A2, the Q-value was reproduced. Due to an accidental vacuum breakdown, the Q-value deteriorated at the end of the period B2. It was gratifying to note that after warming up, pumping and cooling down again, the high field Q was restored.

From Q-dependence on field (Fig. 8) one would expect equal breakdown characteristics in periods A1 and B3, but this is not the case. Thermal breakdown occurred at $\Delta f = 600$ kHz in period A1, whereas no thermal breakdown was seen up to $\Delta f = 994$ kHz in period B3. Limitation of field strength merely was given by a 19 Hz mechanical oscillation enhanced by ponderomotive forces, as described in Sec. 4.3. Though the upper limit of cooling capacity for the helices should be $P_c = 3.25$ W,[25] rf power up to 7 W could be fed to the resonator during period B3, in the 103 MHz mode even more than 25 W. A thermometer on the bottom of the outer cylinder showed a temperature rise with rf

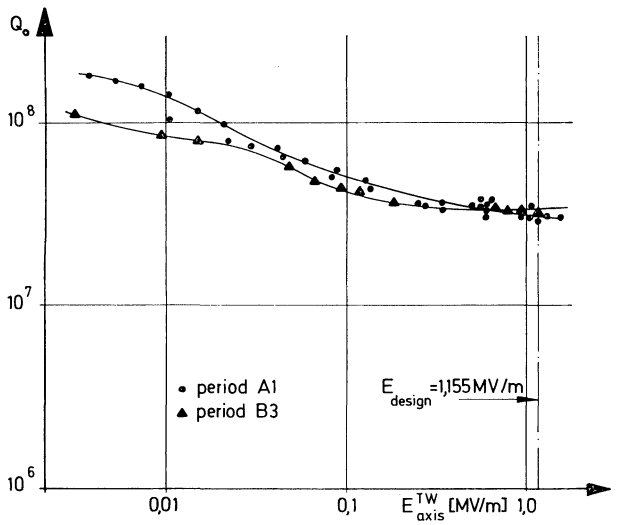

FIG. 8. Results of Q_o-measurements on the first helix section as function of accelerating field strength on the axis.

power and instabilities were seen at a cavity power exceeding 4 W approximately. We concluded from this that the predominant losses in period B3 occurred either on the cylindrical part of the outer conductor or, more likely, in the joint to the niobium 'Deckel'.

The design value of $E^{TW}_{axis} = 1.155$ MV/m corresponds to a static frequency shift $\Delta f = 690$ kHz according to Eq. (3). In periods A1 and A2 power levels corresponding to $\Delta f = 600$ kHz could be handled in stable operation, giving nearly the design field. In the second experimental run (B1–B3) the initial limitation of field strength by ponderomotive oscillations could be overcome using a coupling between frequency and amplitude controls as described in Sec. 4.3. In this way stable operation for hours was obtained at the design field during period B3; at a maximum frequency shift of $\Delta f = 994$ kHz stability still persisted. This corresponds to an accelerating field on the axis of $E^{TW}_{axis} =$ 1.4 MV/m and peak fields of $E_z^p = 18$ MV/m and $H_r^p = 530$ G.

Field emission started at peak fields of about 14 MV/m. The additional load was so low even at 18 MV/m, that no influence on the measured cavity Q-value could be seen. The enhancement factor from a Fowler-Nordheim plot was 320, measured in period B3.

The phase error between adjacent helices was smaller than 0.1° at an external vibration level of 24 kHz_{pp} (period A1) and smaller than 0.4° at an enhanced vibration level of 150 kHz_{pp} (period B3).

4.3. *Frequency and Amplitude Control System*

The question of frequency and amplitude stability of the helix resonator is strongly connected with the operation of the rf control system. In general, the operation of the rf control system was satisfactory in the first experimental run (periods A1 and A2). Improvements on the circuit have been made preceding period B1.

Many difficulties arose from the fact that the influence of ambient vibrations on the modulation of the cavity frequency (fm) exceeded by far the effects known from laboratory experiments. Therefore, a major interest was dedicated to investigations of ambient vibrations. In general during periods A1 and A2, the frequency swing of the first helix section varied between 20 kHz and 100 kHz (peak to peak). That time the cryostat was bolted to a large concrete block which, in turn, rested on the floor. Auxiliary measurements of mechanical perturbation amplitudes indicated that the horizontal vibrations were amplified by a factor of 7 between the concrete block and the top of the cryostat. Therefore, a provisional mechanical insulation from the floor was installed at the cryostat preceding period B1. Then the frequency swing was reduced to a range between 10 kHz and 14 kHz (peak to peak). A basic fm amplitude of 3 kHz remained

after turning off all external equipment (pumps, refrigerator etc.). These results must be seen in view of the general problem of controlling the frequency of a cavity with a given Q and power consumption P_c. It can be shown on general principles that the control element (fast tuning device) must handle a reactive power of $P_r = (\Delta f_{pp}/f_0) \times P_c Q_0'$. For several reasons, one would like to have $P_r < 3$ kVA which, for the parameters of the present cavity, implies a fm of less than 2.2 kHz (peak to peak). Therefore, it is clear that a great deal more attention must be given to vibration insulation.

Properties of frequency and amplitude controls were investigated to handle the electromagnetic-mechanical interactions in the coupled array of helices. An important result is that this cavity behaved very much like a single helix cavity. In the two experimental runs the ponderomotive effects could be handled finally up to the design field strength and higher. First in period B1, the obtainable field strength was limited at relatively low power levels.

A 19 Hz mechanical oscillation could not be influenced by the feedback system if the rf power exceeded a certain limit and led to instability. This situation could be overcome in periods B2 and B3 up to $\Delta f = 1$ MHz. This was possible by inserting an additional loop using the phase error signal and acting on the generator amplitude (variable amplifier in circuit diagram Fig. 2). The additional coupling with variable amplifier can be used only as alternative to an amplitude feedback system (Fig. 2). This coupling has been studied in detail and will be described elsewhere.[34] At higher field levels, above $\Delta f = 1$ MHz, again no stable operation was possible, because then the compensation coupling was not strong enough any longer.

To determine the closed loop gain of the frequency feedback system, a sinusoidal perturbation of variable frequency f_{LF} was applied to the VCO frequency control input (Fig. 2). The resulting change in the output of the frequency control unit was measured as a function of f_{LF}. The unity gain frequency was determined to be about 40 kHz from the experimental data[35] (see Fig. 9). The loop gain shows a 40 dB/decade decay below unity gain frequency, which is in agreement with theoretical considerations. Below 150 Hz the loop gain was not measurable.

To get a better understanding of the whole system, measurements of the 'effective' bandwidth

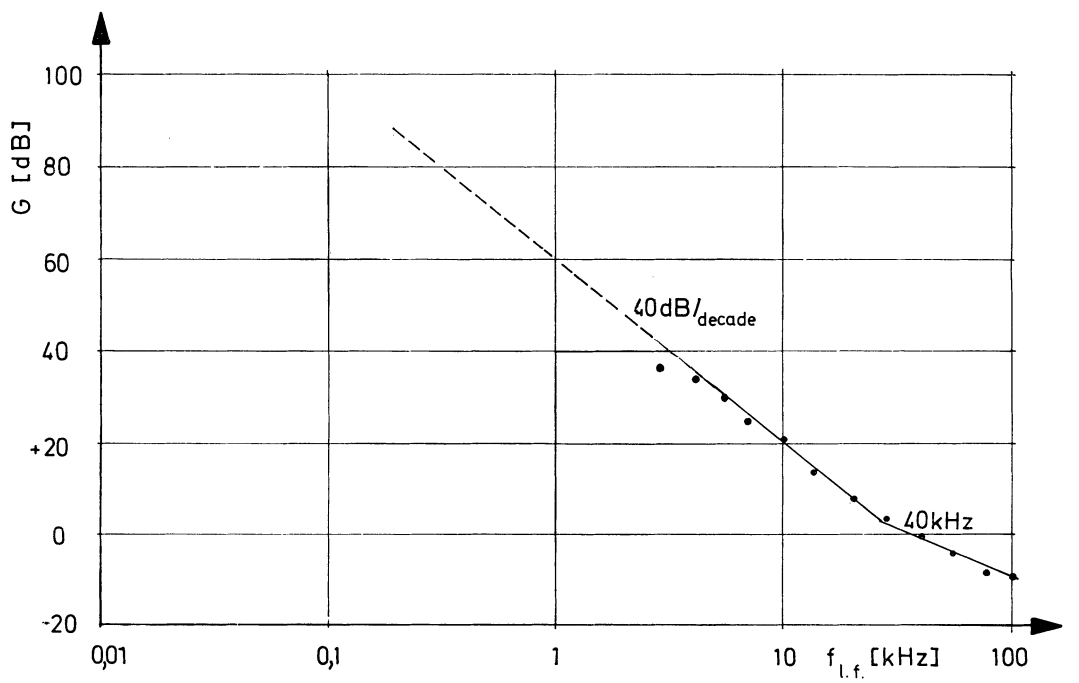

FIG. 9. Loop gain G of the frequency feedback system as function of perturbation frequency $f_{l.f.}$.

of the frequency controlled system were carried out. While the uncontrolled system is determined by the well known asymmetric resonance curve (Fig. 10, curve I), frequency feedback acts like the lines in Fig. 10 (curves II and III). The curves do not exist on the low frequency side of the resonance; they can be realised only up to the resonance point.

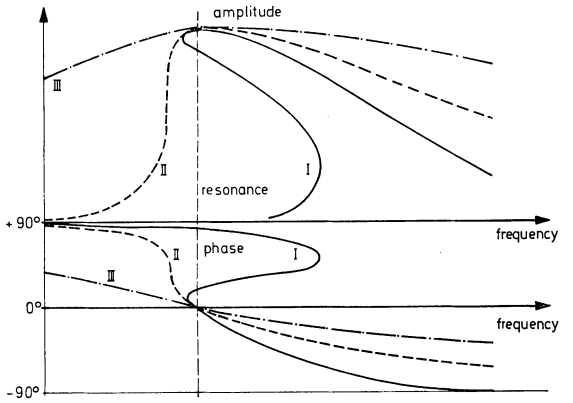

FIG. 10. Schematic drawing of the static resonance curve of a superconducting helix, without frequency feedback (I), with low (II) and with higher loop gain frequency feedback (III).

This was verified observing the remaining phase error signal as function of an external frequency perturbation fed to the VCO input. Stable operation is possible only on the lower frequency side of the resonance curve, as observed before in single helix experiments.

Further, the gain-frequency curve of the amplitude feedback system was measured.

Amplitude stability was tested observing the power levels at various coupling probes. At the reference probe for the feedback system, the variation of amplitude was unobservable on an oscilloscope implying regulation to at least 1 per cent.

Finally, the frequency shift due to electromechanical forces of the coupled array of 5 helices is the expected one (see Sec. 4.2). If individual helix sections can be operated inside a certain range of field levels, then the strong dependence of frequency on field level can be used as a gross tuning device, possibly eliminating the need for 'slow' mechanical tuners.

4.4. *Operation of the Cryogenic System*

In periods A, the cryostat was cooled down for the first time by the refrigerator and operated at 1.8 K.

Due to the wrong dimensioning of a diaphragm the cryostat had to be operated in the batch mode where helium is supplied at intervals, followed by pumping to maintain constant temperature. The cycle time was short, about 2 hours for running and 2 hours for filling, which proved to be a disadvantage in the rf measurements.

These difficulties were eliminated for the experimental runs B. Now the cryostat could be operated in a continuous mode, i.e., helium was continuously supplied by the refrigerator.

The operation of the cryogenic system can be summarized as follows: Starting refrigerator and cryostat at room temperature the cooldown takes about 15 hours to get liquid helium (4.2 K) into the twin pipes, and another 15 hours to fill them up with 1.8 K helium. After about 50 hours from the beginning thermal equilibrium in the Nb 'Deckel', the helices and the quadrupole doubled is established, i.e., they are filled with liquid helium and the resonator can be operated with several watts rf power.

The vacuum system was checked before cooldown. From room temperature to 4.2 K we did not find any leak in either vacuum system. The ultrahigh vacuum at 4.2 K was better than 10^{-10} Torr, and the isolation vacuum at 4.2 K was better than 10^{-6} Torr (which was the sensitivity limit of the Penning gauge). After passing the λ-point an integral superleak of about 4×10^{-2} Torr liters/sec suddenly appeared in the isolation vacuum. The gas pressure rose to 7×10^{-5} Torr, which influenced the ultrahigh beam vacuum. This is due to the diffusion flanges used; this influence possibly can be eliminated with better UHV-flanges. Thus the beam vacuum was in the 10^{-7} Torr range. The process is reversible warming up above the λ-point. The leak rate was the same in periods B, though all gaskets had been replaced. The leak seems to be at a weld, but all efforts to locate it at room temperature failed. The relatively high leak rate was not troublesome in any way, due to the double-vacuum principle.

An unexpected difficulty was the temperature measurement of the cold parts in vacuum by means of carbon resistors. Although the resistors were contacted very thoroughly and the thin Cu-Ni connecting wires were thermally bonded at the helium pipes twice, the experimentally measured

absolute T-values were wrong by several degrees. This was due to an unpermissible flux of heat to the carbon resistors, which results from the 77 K radiation of the LN_2 shield on the unprotected connecting wires.

4.5. *Experiments with the Proton Beam*

Accelerator experiments could be done only with a dc beam up to now, because the buncher could not be used (see Sec. 2.2). In these first experiments the proton beam current was limited, because the rf coupling factor of the superconducting cavity was too small. With the presently existing coupling probes only a beam power up to 10 W can be handled. This corresponds for a bunched beam to a beam current of about 25 μA at the designed energy gain of 368 keV ($\phi = -30°$) in this section. The construction of the rf coupling probes will be changed for future experiments.

The energy gain as function of field strength in the helix resonator and injection energy was measured. The results are summarized in Fig. 11. A computer program was used to recalculate the accelerating field from the measured energy gain. This program uses the field pattern on the axis of the accelerating section as measured by perturbation measurements at room temperature. Measured and calculated values are compared in Fig. 11. The measured values fit well to the calculated ones. A maximum energy gain of 380 keV at the designed field strength of 1.155 MV/m was obtained with the dc beam at an injection energy of 750 keV. An energy gain of 452 keV was obtained at a field of 1.35 MV/m. The experimental error in T_{total} was about 5 per cent (period A2), and about 10 per cent (period B3), respectively. The energy gain of the accelerating section is 10 per cent lower, only, at injection energies of 700 keV and 800 keV (Fig. 11).

A continuous test with the dc beam was carried out in period B3. A field level of 1.3 MV/m was maintained within the superconducting structure for 3.5 hours. A dc beam with low current was accelerated and detected at the cryostat exit. We used no rf amplitude control system that time. Therefore, the injected beam current was set to 1.3 μA due to instabilities in the ion source of the preinjector.

Some tests on nonresonant beam loading phenomena were done according to a method from

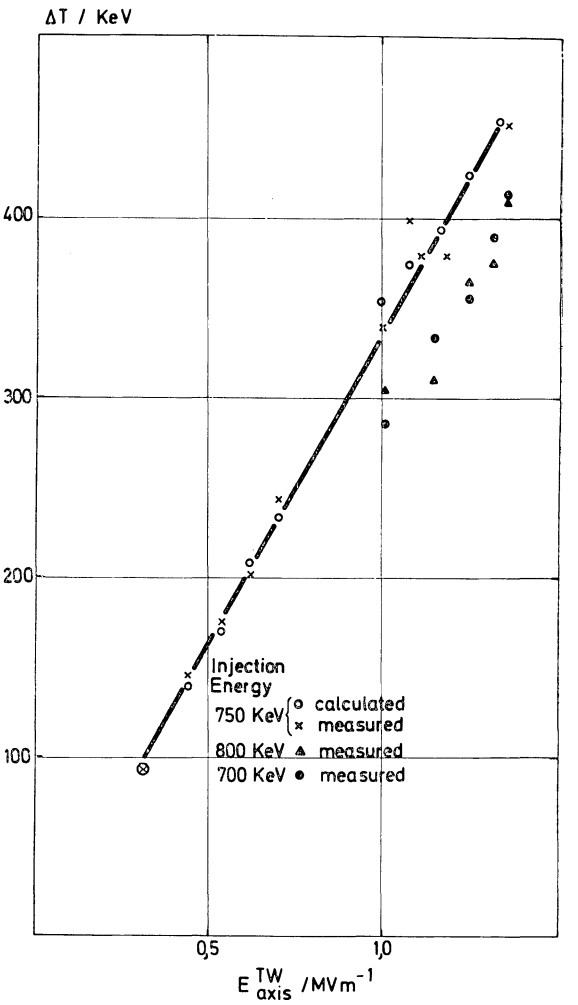

FIG. 11. Results of energy gain measurements for a continuous proton beam. Energy gain versus electrical field strength on the axis at different energies.

an early electron analog experiment.[36] The results are still qualitative and must be completed by further measurements. In the 94 MHz- and 103-MHz-mode no excitation up to proton currents of 0.5 mA could be seen as expected. The phase velocities of all other modes are higher than the phase velocity in the π-mode, which is equal to the particle velocity at an injection energy of 750 keV. The rf power fed to the cavity was practically zero in this measurement (a very low rf power level was used for detection purposes). No rf signal from the cavity could be detected due to excitation by the unpulsed proton beam.

The operation of the proton injector indicated that improvements on the stability of the proton current at very low intensities are necessary. In addition, the beam line geometry is affected, changing the cathode of the duoplasmatron source.

Finally, the properties of the superconducting quadrupole doublet were investigated with the proton beam. A fraction of the quadrupole aperture (60 mm) of about 26 mm in diameter could be illuminated with a beam that was focussed on a hole of 0.5 mm diameter at the entrance of the cryostat. Emittance measurements at the cryostat exit were carried out from which the error in magnetic gradient can be deduced. Agreement with field measurements of this quadrupole doublet on a magnetic measuring machine[37] is found within the error limits. However, both results are incomplete with respect to the larger aperture of the quadrupole and must be completed by future experiments. In addition, from the field measurements the effective magnetic length of the quadrupoles has been determined to be 9.4 cm each, and the calibration factor of 46.6 G/cm/A was obtained.

5. CONCLUDING REMARKS

A first step was done towards the objectives of the Karlsruhe accelerator program. In two independent experimental runs a proton beam has been accelerated to the designed energy gain within the first section of the superconducting helix accelerator. Reproducible Q-values have been obtained. It has been demonstrated that a vacuum failure does not cause an irreversible deterioration of the Q-value.

The order of magnitude of Q is still comparatively low. An improvement factor of 2×10^4 would be at the lower economic limit[12] for a larger superconducting accelerator, but for a pilot linac this is not essential. Future improvements can be expected. Another important result is the fact that mechanical instabilities and ponderomotive interactions of a coupled array of 5 helices have been handled in stable operation. In addition, the parameters of the necessary rf feedback system have been studied in detail. Moreover, the cryogenic system with the cryostat for superfluid helium has proved to be satisfactory, and long-term operation with the helium refrigerator functioned properly.

The next step will be the operation of two independent superconducting helix sections. Then, different from the rf system used so far, the second section has to be operated at a frequency given by the first section. For this reason, the second helix section will be equipped with a stronger rf coupling and an external load to broaden the bandwidth. Alternatively, a dynamic frequency tuner can be used on a transmission type resonator with the same type of coupling. The preparations for this next extension of the superconducting linac have started already, some time ago.

ACKNOWLEDGEMENTS

The execution of the whole program would not have been possible without the help of many people involved in the linac work at Karlsruhe. The authors are indebted to J. Halbritter for assistance and many helpful discussions. P. Kneisel and O. Stoltz created the basis for the preparation of the superconducting surfaces by their work on superconducting resonators. The realization of the first helix section was mainly done by N. Münch and G. Westenfelder. F. Spath and his crew untiringly ran the refrigerator. W. Herz, F. Schürrer, H. Schittenhelm and R. Vincon did all the mechanical assembly of the cryostat and the cryogenic system, which has been designed and constructed with the help of F. Graf and B. Haferkamp. Responsible for maintenance of the vacuum system was L. Hütten. A. Hornung was involved in the rf measurements; P. Grundel and H. Oppermann were responsible for the operation of the proton injector, G. Redemann installed the chopper/buncher system. The skill and effort of the mechanical workshop under R. Boehmer made it possible to adhere to a tight schedule.

REFERENCES

1. M. S. McAshan, H. A. Schwettman, L, Suelzle, and J. P. Turneaure, High Energy Physics Laboratory Report 665, Stanford, January 1972.
2. A. O. Hanson, *IEEE Trans. Nucl. Sci.* **NS-18,** No. 3, 149 (1971).
3. A. J. Sierk, C. J. Hamer, and T. A. Tombrello, *Part. Acc.* **2,** 149 (1971).
4. R. Benaroya, A. H. Jaffey, K. Johnson, T. Khoe, J. Livingood, J. M. Nixon, G. W. Parker, W. J. Ramler, J. Aron, and W. A. Wesolowski, *Appl. Phys. Letters* **21,** 235 (1972).
   A. Moretti, J. W. Dawson, J. J. Peerson, R. M. Mill,

M. T. Rebuehr, *IEEE Trans. Nucl. Sci.* **NS-18**, No. 3, 186 (1971).
5. C. M. Jones, J. P. Judish, R. F. King, F. K. McGowan, W. T. Milner, and P. Z. Peebles Jr., *Part. Acc.* **3**, 103 (1972).
6. J. P. Turneaure, *Appl. Phys. Letters* **16**, 333 (1970); and *IEEE Trans. Nucl. Sci.* **NS-18**, No. 3, 166 (1971).
7. P. B. Wilson, M. A. Allan, H. Deruyter, Z. D. Farkas, H. A. Hogg, E. W. Hoyt, H. L. Martin, and M. Rabinowitz, *Proc. 8th Int. Conf. High Energy Accelerators, CERN, Geneva, 1971*, p. 238.
8. M. Boussoukaya and A. Septier, *Part. Acc.* **2**, 315 (1971).
9. H. J. Halama, *IEEE Trans. Nucl. Sci.* **NS-18**, No. 3, 188 (1971); and *Part. Acc.* **2**, 335 (1971).
10. P. Kneisel, O. Stoltz, and J. Halbritter, *IEEE Trans. Nucl. Sci.* **NS-18**, No. 3, 158 (1971); and *Proc. Appl. Superconductivity Conf., Annapolis, May 1972*, p. 657.
11. E. A. Knapp, *IEEE Trans. Nucl. Sci.* **NS-18**, No. 3, 508 (1971).
12. H. Klein and M. Kuntze, *IEEE Trans. Nucl. Sci.* **NS-19**, No. 2, 304 (1972).
13. A. Citron, *Proc. 1970 Proton Lin. Acc. Conf., Batavia 1970*, Vol. I, p. 239.
14. H. Klein, N. Merz, and O. Siart, *Part. Acc.*, to be published.
15. K. W. Zieher, *Nucl. Instr.*, to be published.
16. A. Schempp, Univ. Frankfurt, Int. Report No. 12, March 1971.
17. D. Schulze, *Proc. 1970 Proton Lin. Acc. Conf., Batavia 1970*, Vol. I, p. 359.
18. D. Schulze, Karlsruhe, KFK-Bericht 1493, Dec. 1971.
19. D. Schulze, S. Brandelik, R. Hietschold, G. Hochschild, A. Hornung. F. Spielböck, and L. Szecsi, to be published at Los Alamos Conf., Oct. 1972.
20. D. Schulze, H. Strube, K. Mittag, B. Piosczyk, and J. E. Vetter, *IEEE Trans. Nucl. Sci.* **NS-18**, No. 3, 160 (1971).
21. M. Kuntze, *IEEE Trans. Nucl. Sci.* **NS-18**, No. 3, 137 (1971).
22. W. Baldus, *Proc. Cryogenic Eng. Conf. Boulder 1970*, p. 163.
23. P. Flécher, *J. Vac. Sci. and Tech.* **9**, 46 (1971).
24. W. Barth, P. Flécher, F. Graf, M. A. Green, W. Herz, L. Hütten, H. Katheder, W. Lehmann, F. Spath, and G. Winkler, *Proc. 4th Int. Cryog. Eng. Conf. ICEC 4, Eindhoven, May 1972.*
25. G. Krafft, *Proc. 4th Int. Cryog. Eng. Conf. ICEC 4, May 1972*: and Karlsruhe, KFK-Report 1584, April 1972.
26. P. Flécher and R. Vincon, *Vakuum Technik* **20**, 135 (1971).
27. J. L. Fricke, B. Piosczyk, J. E. Vetter, and H. Klein, *Part, Acc.* **3**, 35 (1972).
28. A. Citron, J. L. Fricke, C. M. Jones, H. Klein, M. Kuntze, B. Piosczyk, D. Schulze, H. Strube, J. E. Vetter, N. Merz, A. Schempp, and O. Siart. *Proc. 8th Int. Conf. High Energy Accelerators, CERN, Geneva, Sept. 1971*, p. 278.
29. O. Siart, Dissertation, Univ. Frankurt/M. (1970)
30. A. Schempp, Univ. Frankfurt, Internal note.
31. H. Martens, H. Diepers, and R. K. Sun, *Phys. Letters* **34A**, 439 (1971).
32. P. Kneisel, O. Stoltz, J. Halbritter, H. Diepers, H. Martens, and R. K. Sun, *Proc. 8th Int. Conf. High Energy Accelerators, CERN, Geneva*, p. 275, Sept. 1971.
33. J. Halbritter, *Part. Acc.* **3**, 163 (1972).
34. D. Schulze, Karlsruhe, KFK-Report, to be published.
35. A. Hornung, Karlsruhe KFZ, Internal report.
36. K. Mittag, M. Kuntze, F. Heller, and J. E. Vetter, *Nucl. Instr. and Meth.* **76**, 245 (1969).
37. J. Brandes, G. Friesinger, and A. Ulbricht, Karlsruhe, KFK-Report 1220, May 1970; and J. Brandes, A. Ulbricht, Karlsruhe, KFK-Report 1644, Aug. 1972.

Received 14 September 1972